Progress in Earth and Planetary Science
a SpringerOpen Journal

RESEARCH Open Access

Distribution of U and REE on colloids in granitic groundwater and quality-controlled sampling at the Mizunami underground research laboratory

Takashi Munemoto*, Kazuaki Ohmori and Teruki Iwatsuki

Abstract

Colloids and their association with analogue elements, uranium, and rare earth elements (REEs), in deep granitic groundwater were investigated at the Mizunami Underground Research Laboratory (MIU). Groundwater was sampled from underground boreholes and gallery walls, and the colloids were separated by size-fractionated ultrafiltration (pore sizes, 0.2 μm, 10 kDa, and 1 kDa). For the groundwater sampled from fractures in excavation walls, the size-fractionated concentrations of the colloid-forming elements were approximately constant relative to different size fractions (0.2 μm, 200 kDa, 50 kDa, and 10 kDa). The contamination of Fe- and Al-bearing materials was insignificant in the filtered groundwater from fracture seepages. Changes in the concentrations of U in the groundwater sampled from boreholes and excavation walls were associated with the Al-bearing colloids, Fe-bearing colloids, and organic matter. The REE-bearing material(s) that were >0.2 μm in size were mobile in the deep granitic groundwater, rather than occurring in association with Al-bearing, Fe-bearing colloids, and organic matter. It is suggested that sampling from water-conducting fractures in host rock and colloid elimination in borehole are important components of water quality control in geochemical investigations.

Keywords: Mizunami Underground Research Laboratory; Colloid-facilitated transport; Quality-controlled sampling; Deep granitic groundwater; Rare earth elements; Uranium

Background

Colloid sampling procedures in groundwater are an important aspect of groundwater research. Sampling of groundwater and colloids is often conducted in vertical or near vertical boreholes or wells drilled from the ground surface. However, the artesian pressure in groundwater may decrease to atmospheric pressure, and the *in situ* oxidation-reduction condition of the groundwater may change during sampling. Furthermore, the subsurface environment may become contaminated by drilling fluid, artifacts such as steel drill bits and rods containing Fe, and meteoric water during drilling (Dideriksen et al. 2007). Changes in the chemical composition and physicochemical condition of groundwater may induce the formation of anthropogenic colloids and secondary minerals, especially Fe(III)-(oxy)hydroxides. The chemical composition of groundwater may be affected by co-precipitation and sorption of elements onto newly formed colloids and secondary minerals.

Groundwater sampling in an underground research laboratory (URL) is advantageous for *in situ* sample collection. *In situ* groundwater and colloid sampling techniques that are capable of maintaining artesian pressures and anaerobic conditions have been developed at the Mizunami Underground Research Laboratory (MIU) in Mizunami, Gifu Prefecture, Japan (Aosai et al. 2010). However, the effect of the presence of anthropogenic colloids and secondary minerals on groundwater chemistry remains unclear due to sampling difficulties. We have observed anthropogenic secondary minerals on borehole walls using a borehole televiewer (BTV) in boreholes drilled into granitic rock. Although the granite is fresh immediately after drilling, BTV photographs taken in different boreholes [09MI20 (Figure 1a) and 10MI26 (Figure 1b) details in the *Sampling from boreholes* section] show that

* Correspondence: munemoto.takashi@jaea.go.jp
Mizunami Underground Research Laboratory, Geoscientific Research Department, Sector of Decommissioning and Radioactive Waste Management, Japan Atomic Energy Agency, 1-64 Yamanouchi, Akeyo, Mizunami, Gifu 509-6132, Japan

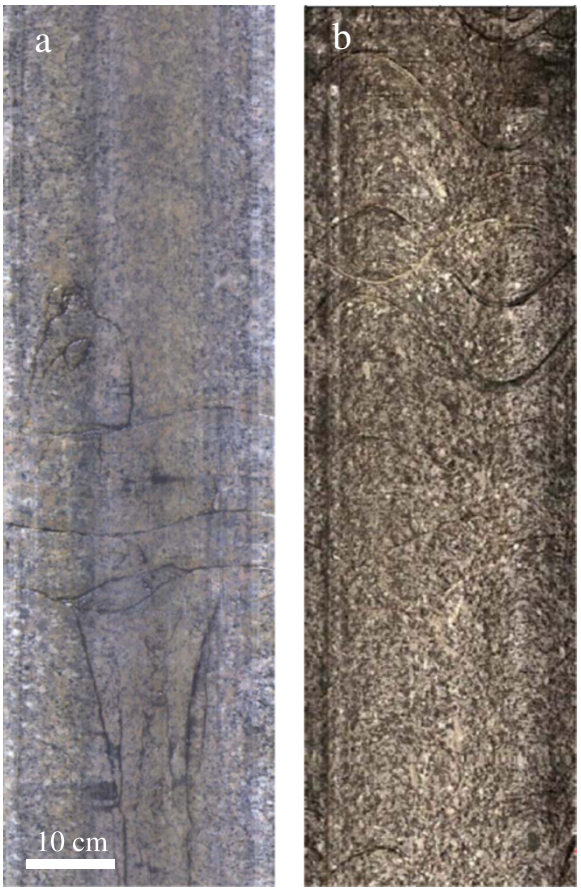

Figure 1 BTV photographs of the boreholes (a) immediately after drilling the 10MI26 borehole and (b) several days after drilling the 09MI20 borehole.

an anthropogenic blackish precipitate has developed on the borehole wall several days after drilling (Figure 1b).

We have conducted groundwater and colloid sampling by ultrafiltration using different pore size membrane filters. The distributions of analogue elements, especially U and rare earth elements (REEs), onto colloidal material in deep granitic groundwater are presented herein. Based on the results of ultrafiltration, the present study discusses the effect of colloids on groundwater chemistry and proposes technical methods for quality-controlled groundwater and colloid sampling.

Colloids and nanoparticles

Colloids and nanoparticles (generally defined as particles of <1 μm in diameter) are widespread throughout the Earth's surface, in sediments, soil, rivers, oceans, and groundwater (Sholkovitz et al. 1994; Degueldre et al. 2000; Hochella et al. 2008). Mineral colloidal particles, Al/Fe-(oxy)hydroxides, clays, and carbonates, and biological organic colloids have been observed in natural systems (Filella et al. 2009). The predominant sources of the colloids and nanoparticles are (1) the mobilization of colloidal materials from source rock and sediments and (2) the precipitation of supersaturated mineral phases depending on the solubility and solution conditions (Ryan and Elimelech 1996).

The mobilization of colloids and nanoparticles is triggered by chemical disturbance such as changing solution pH, ionic strength, and surface charge of colloids and nanoparticles, and physical disturbances, such as rapid infiltration and groundwater flows. The mobility of the particles in water is very complicated depending on their genesis, dispersion, and aggregation (McCarthy and Zachara 1989). The removal of colloids and suspended particles from solution has been conducted by ultrafiltration by using a 0.45 or 0.2 μm membrane (Buddemeier and Hunt 1988). However, the colloidal materials often passed through the membrane (Pokrovsky et al. 2010), while aggregates of very fine nanoparticles (5 to 7 nm) can be trapped on the membrane (Tsubaki et al. 2012). The sedimentation velocity of particles in solution is dependent on their size (Tsukimura et al. 2010). Large particles settle rapidly, whereas nanoparticles scarcely settle. In natural systems, aggregation of nanoparticles makes estimating sedimentation velocity difficult because the particle size changes with aggregation (Flury and Qiu 2008). When colloids are strongly attached to source rock and/or settle by aggregation, they are immobile. The primary physical disturbance causing colloid mobility is an increase in the water flow velocity by pumping and/or fluctuation of hydraulic pressure. Due to such physical disturbances, naturally immobile colloids are mobilized in aqueous systems.

The interaction between minerals and water induces the dissolution of primary minerals and the precipitation of secondary minerals and nanoparticles. The formation of secondary minerals and colloids is dependent on solubility. For example, aqueous Fe easily precipitates from solution under oxidizing conditions and a wide range of pH conditions because of the extremely low solubility of Fe-(oxy)hydroxides (Stefánsson 2007). In addition to Fe-bearing colloids, the solubility of toxic elements and radioactive nuclides is very low under reducing conditions (Neck and Kim 2001). Intrinsic colloids consisting of radionuclides have been observed in groundwater, in which they occur as oxides and hydroxides (Kersting et al. 1999). It is important to understand the mobility of colloids and nanoparticles associated with the mobility of pollutants and radionuclides, especially for the evaluation of safe storage and disposal of nuclear waste.

Interaction between the liquid phase and colloid particles

Colloids and nanoparticles have large surface areas, high sorption capacity, and transport ability for sorbing aquatic components (Kersting et al. 1999; Novikov et al.

2006; Wang et al. 2013). Various laboratory experiments involving the sorption of elements onto colloids and nanoparticles have been conducted (Waite et al. 1994; Mahoney et al. 2009). Fe (oxy)hydroxide (ferrihydrite) is one of the most important colloids in the natural environment for the transport of elements (Raiswell 2011). Experiments to examine sorption onto ferrihydrite have been extensively investigated with regard to both cations and anions (Dzombak and Morel 1990).

In natural environments, it has been reported that hydrous ferric oxide nanoparticles sorbing U and Pu have been transported for great distances in groundwater at the Mayak Production Association in Russia (Novikov et al. 2006). Kersting et al. (1999) have reported that Pu and fission products in groundwater have been observed 1.3 km from the location of explosions at the Nevada Test Site in the United States. The mobility of Pu and fission products could be facilitated by colloidal materials. The variety of the colloidal material at the site has been characterized as including uranate, phosphates, silicate, and metallic aggregates (Utsunomiya et al. 2009).

The sorption capacity of colloids is dependent on surface properties, which can vary with solution conditions, such as pH and ionic strength (Davis and Kent 1990). Clay minerals, such as illite and smectite, are also important sorbents in the natural environment, which can scavenge several toxic metals by adsorption and ion exchange (Opiso et al. 2009). Abdel-Fattah et al. (2013) investigated the stability of intrinsic Pu colloids with smectite clay colloid in solution and showed that the intrinsic Pu colloids can be transported in association with stable smectite clay colloids. Aqueous components can move a considerable distance in the subsurface if they are sorbed and attached onto mobile colloids and nanoparticles (Kersting et al. 1999; Buddemeier and Hunt 1988). This phenomenon is referred to as colloid-facilitated transport by McCarthy and Zachara (1989). Thus, colloids and nanoparticles can significantly affect the subsurface transport of elements.

U and REEs in groundwater

Uranium is one of the most important elements of concern with regard to the safe storage and disposal of nuclear waste. In natural conditions, the redox states of U are insoluble tetravalent [U(IV)] and soluble hexavalent [U(VI)]. The mobility of dissolved [U(VI)] associated with colloids has been observed in the natural environment (Claveranne-Lamolère et al. 2011). The adsorption of U onto colloids is highly dependent on water chemistry. For example, the adsorption of U onto Fe-(oxy)hydroxide is dependent on dissolved U species (Waite et al. 1994). In contrast to the hexavalent state, tetravalent U oxide (uraninite, UO_2) is highly stable and insoluble, and its formation results in the immobilization of U under reducing conditions (Metcalfe et al. 2006). Most recently, Wang et al. (2013) investigated mobile U(IV) associated with Fe and organic colloids in reducing pore water.

The chemical properties of trivalent REEs, especially those for light REEs (LREEs) are comparable to transuranic elements in high-level radioactive waste, americium (Am), and curium (Cm) due to similarities such as ionic radius, oxidation state, and complexation of anions (Krauskopf 1986). In addition, REEs are used in industrial processes, and these are anthropogenically released to river water (Kulaksız and Bau 2013). The mobility of REEs is affected by rock-water interactions, such as the dissolution of source minerals and the adsorption and incorporation on/into secondary minerals (Bau 1999; Coppin et al. 2002; Willis and Johannesson 2011). In natural environments, relative abundances of REEs in minerals and water are widely used as a geochemical tracer of water-rock interaction. For example, in the Tono area, Japan (detailed in the site description section), the REEs in groundwater are leached from granitic source rock deep underground and transported to shallow sedimentary rock by groundwater flow (Takahashi et al. 2002). Many studies have focused on the mobility of REEs associated with colloidal materials (Sholkovitz 1992; Dia et al. 2000; Willis and Johannesson 2011). The distribution of REEs and U onto colloids is complex because it depends on the colloidal and aqueous species, which vary with aquatic conditions such as pH, Eh, and ionic strength. The quantitative estimation of the distribution of U and REEs on colloids in natural groundwater is analogous to colloid-facilitated transport in the safe storage and disposal of waste.

Site description of the MIU

Around the MIU construction site in the Tono area, sedimentary rocks of the Seto Group (12 to 1.5 Ma) and the Mizunami Group (20 to 15 Ma) unconformably overlie the basement rock, i.e., the 70 Ma Toki Granite (Sasao et al. 2006). The Toki granite has been classified into three zones by Iwatsuki and Yoshida (1999) based on the intensity of fracturing and fracture widths: an intact zone, a moderately fractured zone, and an intensely fractured zone. The intact zone is characterized by relatively few fractures, which have kaolinite-, calcite-, and chlorite-filling minerals. The moderately fractured zone has relatively thin fractures with minor alteration of the rock matrix, and the dominant fracture-filling minerals are smectite and chlorite. The intensely fractured zone is strongly altered, and matrices are replaced by kaolinite and smectite. In fractured geologic media, groundwater flow and transport are affected by the density and properties of water conducting fractures (Tsang et al. 1990). In the Toki granite, groundwater moves through the fractures along water flow paths (Illman et al. 2009). The

baseline groundwater chemistry was determined through surface borehole investigations prior to MIU construction. The groundwater is Na-Ca-HCO_3 type in the upper sedimentary rock formations, which is a result of water-rock interaction. In the deeper sedimentary rock and the basement granite, Na-(Ca)-Cl type groundwater occurs, which may be derived from a paleo-hydrothermal water or from fossil sea water recharge in the Miocene (Iwatsuki et al. 2005).

Construction of the MIU is being conduced by the Japan Atomic Energy Agency (JAEA). By 2013, the MIU facilities had been excavated to 500 m below ground level (mbgl). The underground facilities consist primarily of the main shaft and a ventilation shaft, There are sub-stages at 100 m intervals connecting the two shafts, and the two research galleries at 300 and 500 mbgl (Figure 2a). Three horizontal boreholes, 07MI07, 09MI20, and 10MI26, were drilled into granite at the −200, −300, and −400 sub-stages, respectively. Each borehole has been divided into six sampling sections using hydraulic packers. Hydrochemical monitoring systems are installed in the boreholes (Figure 2b). These enable sampling of groundwater under anaerobic and *in situ* pressure conditions and are used to measure physico-chemical parameters (temperature, pH, Eh, and water pressure).

A preliminary study by Saito et al. (2013) shows that the major colloids in the MIU groundwater are organic matter, Fe-bearing colloids, and Al-bearing colloids. The analogue elements (REEs and U) in the groundwater were associated with organic matter and Al-bearing colloids. We focus on the effect of the colloid-forming elements, Fe, Al, and total organic carbon (TOC), on the groundwater chemistry. The colloid-facilitated transport of analogue elements by the aquatic colloids is also evaluated.

Methods

Sampling from boreholes

The boreholes used in the present study are separated into six isolated sampling intervals by impermeable packers (Figure 2d). Groundwater was sampled from two sampling intervals, 34.8 to 57.8 m in borehole 09MI20 and 37.9 to 49.6 m in borehole 10MI26, using the installed hydrochemical monitoring system (Figures 2b,d). The sampling interval volumes are 31 and 24 L in 09MI20 and 10MI26, respectively, and the groundwater pressures are 1.7 and 2.7 MPa, respectively. Before opening the groundwater sampling valves in the monitoring system, the groundwater was resident in the sampling intervals. Upon opening the valve, groundwater flowed through a Teflon tube to the outlet with an outflow rate of approximately 1 L/min in both boreholes. The groundwater and colloids were sampled and filtered on site by batch ultrafiltration using 0.2 μm, 10 kDa, and 1 kDa membranes in a stainless steel, pressure-tight filter unit (Millipore, Billerica, MA, USA). The ultrafiltration unit was connected directly to the groundwater sampling outlet tube of the hydrochemical monitoring systems for each membrane pore size. The groundwater passed through the membranes in the filter unit under differential hydraulic pressures between the sampling intervals and the pressure regulators in order to avoid abrupt changes in the hydraulic pressure in each borehole: 1.7 and 1.4 MPa in 09MI20 and 2.7 and 2.4 MPa in10MI26. The groundwater passed through the membranes under inert conditions: almost equal hydraulic

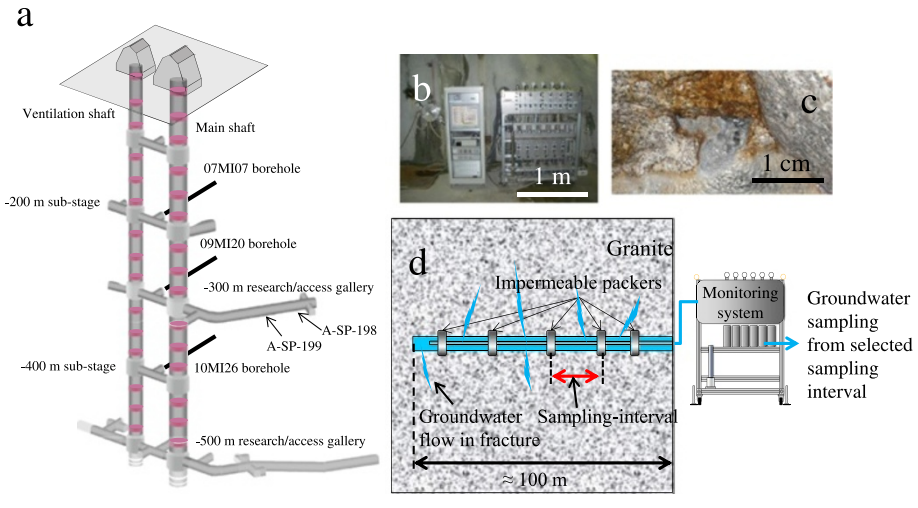

Figure 2 Description of the MIU construction site. (a) Schematic representation of the MIU facilities and sampling sites. **(b)** Groundwater sampling apparatus (photograph taken at the 10MI26 borehole). **(c)** Groundwater seepage from an excavated gallery wall. **(d)** Schematic representation of groundwater sampling from a borehole.

pressures and anaerobic conditions. In addition to the filtered groundwater, unfiltered groundwater was also collected from the boreholes. The size-fractionated samples of 09MI20 and 10MI26 groundwaters were collected in July 2010 and November 2011, respectively.

Blackish precipitation on borehole walls (Figure 1b) may have been randomly flushed from the borehole wall due to water pressure fluctuations during sampling. In order to evaluate the temporal effects of anthropogenic colloids on the chemical composition of the groundwaters from the two boreholes, the initial fluids in the sampling intervals were purged by flushing with fresh groundwater under hydrostatic pressure conditions. Groundwater was sampled after 5, 10, and 20 sampling interval volumes had flowed through in the intervals. The groundwater passed through a 0.2 μm membrane (ADVANTECH, Tokyo, Japan) placed in the filter unit. The groundwater and colloids were sampled on site in October 2012 using the ultrafiltration procedure for size fractionation described above.

Sampling seepage from fractures underground

In addition to groundwater sampling from boreholes, groundwater seepage from fractures in granite was also sampled. Water conducting fractures occur in the −300 m Access/Research Gallery at 79.7 and 44.8 m from the main shaft. The fractures are designated A-SP-198 and A-SP-199 (Figure 2c), respectively. The usual groundwater flow rates from A-SP-198 and A-SP-199 are 1.1 and 15 L/min, respectively. The groundwater seepages from these fractures are at atmospheric pressure and are slightly oxidized. However, groundwater devoid of anthropogenic colloids is expected because man-made disturbances by borehole drilling did not occur. The groundwater seepage from fractures in granite was collected into 5 L stainless steel reservoirs in the gallery. Immediately after sampling, the groundwater was portioned into five Teflon-coated 1 L vessels in the laboratory. Four of the groundwater samples were filtered through 0.2 μm, 200 kDa, 50 kDa, and 10 kDa membranes, and the remaining sample was not filtered and used for estimating the interaction between 'natural colloids' and analogous elements. The molecular weight cutoffs (MWCO) at 200 kDa, 50 kDa, and 10 kDa (ADVANTEC) correspond to pore sizes of approximately 100, 50, and 6.3 nm, respectively (Kanai 2011). The contamination of stainless steel components with Fe, As, and Cr is almost negligible, and the oxidation-reduction potential of the collected groundwater was maintained through ultrafiltration (Aosai et al. 2010). In addition to the filtering of groundwater, we also collected unfiltered groundwater. The concentrations in unfiltered fractions refer to the total content in groundwater, including aqueous components and colloidal material. The groundwater sampling was conducted in September 2012.

Analytical procedure

The physicochemical parameters (temperature, pH, and Eh) of borehole groundwater were measured using a conductivity temperature depth profiler (OceanSeven305, Idronaut, Brugherio, Italy) equipped with hydrochemical monitoring systems maintaining hydraulic pressure and anaerobic conditions. For fracture seepages, the physicochemical parameters were measured on-site using an automated pH meter (D-54 pH meter, HORIBA Ltd., Kyoto, Japan) with a glass electrode (9621-10D) and a pH/ORP meter (D-55 pH meter, HORIBA) with a Ag/AgCl combination Pt electrode (9300-10D). Before the measurements, the pH meter was calibrated with pH 4.01, 6.86, and 9.18 buffers at 25°C, and the ORP meter was checked its function property using saturated quinhydron solution. Immediately after the groundwater samplings, the samples were transferred to a laboratory. The chemical composition of the major elements (Na^+, K^+, NH_4^+, Ca^{2+}, Mg^{2+}, Cl^-, F^-, Br^-, NO_3^-, and SO_4^{2-}) was measured by ion chromatography (ICS-1000, Dionex, Sunnyvale, CA, USA). The concentrations of Si and B were measured by inductively coupled plasma optical emission spectrometry (ICP-OES, CIROS-Mark II, Rigaku, Tokyo, Japan). The TOC analysis was performed using an infrared gas analyzer (NDIR, Analytik Jena, multi N/C 2100S, Analytik Jena, Thuringia, Germany).

Both the filtered and unfiltered groundwaters were acidified with ultrapure HNO_3 and were refrigerated until chemical analyses were performed. The chemical compositions were measured by inductively coupled plasma mass spectrometry (ICP-MS, PerkinElmer, ELAN DRC II, PerkinElmer, Waltham, MA, USA) for Al, Fe, U, and REEs. The concentrations of U and REEs in the groundwater are very low. Both the REEs and U were preconcentrated using a chelating resin disk (Empore Disk Cartridge P/N4371, 3M, MN, USA). The chelating disk was conditioned by sequential injection of 5 mL of 2 M HNO_3, ultrapure water, and a 0.1 M ammonium acetate solution. After conditioning, 40 mL of the groundwater sample was injected onto the chelating disk, and the REEs and U were recovered using 2 mL of 2 M HNO_3. Thus, 102 ± 4% of the concentrated REEs and U were recovered in the preliminary analysis tests. The excess recovery rate may arise from uncertainty in the concentrating technique but it can also be accounted for by the analytical error of ICP-MS (±10%). The morphology and compositions of colloid specimens on the 0.2 μm membrane filter were analyzed by scanning electron microscopy (SEM, HITACHI TD-1000, Hitachi Ltd., Tokyo, Japan) with energy-dispersive X-ray spectrometry (EDS, HORIBA EMAX ENERGY EX-250).

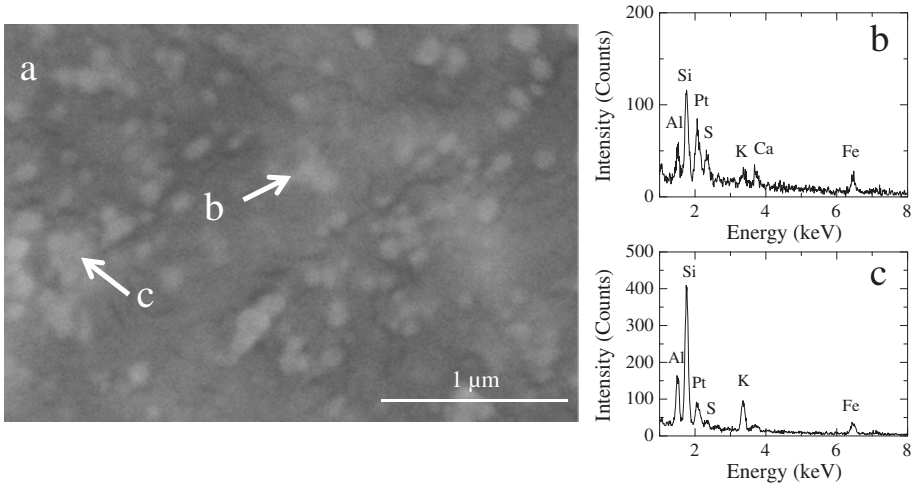

Figure 3 SEM image of colloid collected on a membrane in the 09MI20 borehole. (a) BSE image of the colloid. **(b)** and **(c)** EDS spectra of areas b and c indicated in **(a)**.

Results

SEM observations of colloids in borehole groundwater

The backscattered electron image of the colloids collected in the 09MI20 borehole indicates that they are spherical in shape and have a diameter of approximately 100 nm (Figure 3a). The SEM-EDS examination showed that the particles mainly consist of Si, Al, S, K, Ca, and Fe (Figure 3b,c). Mineralogically, the particles are most likely Fe-bearing aluminosilicates. In the 10MI26 borehole, Fe sulfide, probably pyrite of approximately 1 μm in diameter, and aluminosilicates of several micrometers in diameter were observed (Figure 4).

Groundwater chemistry of major constituents

The major chemical composition of groundwater is provided in Table 1. The chemical compositions of major elements in the filtered groundwater from the 09MI20 and the 10MI26 boreholes obtained by size-fractionated ultrafiltration and groundwater replacement in the borehole were approximately the same as that of the periodically sampled groundwater (although not shown, the data was similar to that presented in Table 1).

The chemical compositions of filtered groundwater should be similar to smaller pore size fractions because colloids and suspended particles in groundwater were basically removed by ultrafiltration. However, the size-fractionated concentrations of Fe in the 09MI20 borehole increased for the smaller membrane pore sizes (Figure 5a). The concentrations of Fe in the 09MI20 groundwater were 52, 16, 40, and 97 μg/L in unfiltered and 0.2 μm, 10 kDa, and 1 kDa filtered groundwaters, respectively. The concentrations of Al in the 09MI20 groundwater

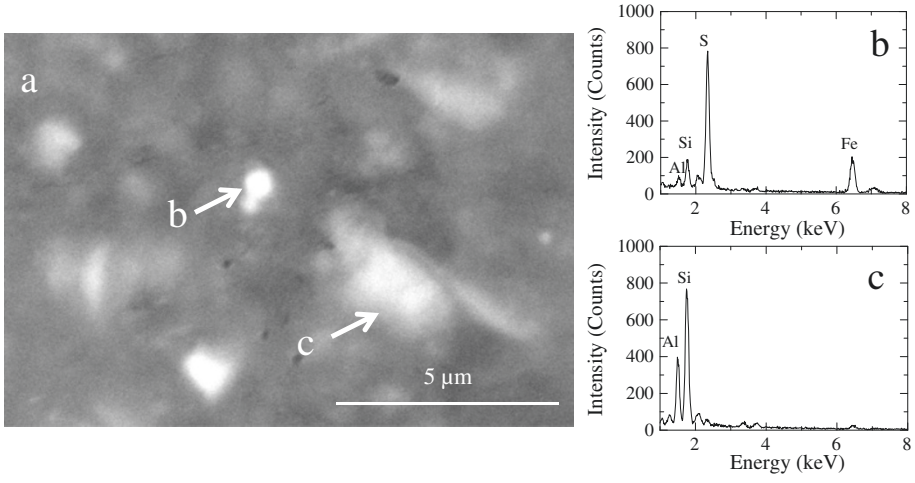

Figure 4 SEM image of colloids collected on a membrane in the 10MI26 borehole. (a) BSE image of the colloid. **(b)** and **(c)** EDS spectra of areas b and c indicated in (a).

Table 1 Average chemical concentration of major elements in the MIU groundwaters

Location	Depth (mbgl)	Packer interval (mabh)	Sampling term	pH	Temperature (℃)	Eh (vs. SHE)	Na^+	K^+	Ca^{2+}	Mg^{2+}	TC	TIC	TOC	Alkalinity	SO_4^{2-}	F^-	Cl^-	NO_3^-	Br^-	NH_4^+	PO_4^{3-}	Si	B
						(mV)	[mg/L]	[mg/L]	[mg/L]	[mg/L]	[mg/L]	[mg/L]	[mg/L]	[meq/L]	[mg/L]	[mg/L]	[mg/L]	[mg/L]	[mg/L]	[mg/L]	[mg/L]	[mg/L]	[mg/L]
07MI07	200	38.7 to 47.2	2010.4.21 to 2012.12.10	8.76 ± 0.15	15.8 ± 5.7	−180 ± 30	82 ± 4	0.4 ± 0.1	12 ± 1	<0.1	14 ± 1	14 ± 1	0.6 ± 0.1	1.2 ± 0.1	13 ± 1	8.9 ± 0.3	77 ± 10	<0.05	0.16 ± 0.05	0.15 ± 0.05	<0.5	6.8 ± 0.1	1.1 ± 0.1
09MI20	300	34.8 to 57.8	2010.4.27 to 2012.12.4	8.44 ± 0.12	19.7 ± 3.9	−110 ± 20	110 ± 7	0.7 ± 0.1	16 ± 3	0.9 ± 0.1	15 ± 1	15 ± 1	0.6 ± 0.1	1.2 ± 0.1	10 ± 1	8.8 ± 0.3	130 ± 20	<0.05	0.23 ± 0.06	0.12 ± 0.04	<0.5	6.7 ± 0.2	1.3 ± 0.1
10MI26	400	37.9 to 49.6	2011.1.15 to 2012.12.5	8.40 ± 0.10	24.1 ± 2.9	−210 ± 30	120 ± 5	0.8 ± 0.1	17 ± 2	0.8 ± 0.1	14 ± 1	13 ± 1	0.6 ± 0.2	1.1 ± 0.1	7 ± 1	8.6 ± 0.3	160 ± 20	<0.05	0.29 ± 0.04	0.12 ± 0.04	<0.5	6.8 ± 0.2	1.5 ± 0.1
ASP-198	300	-	2010.4.2 to 2012.12.18	8.66	22.9	−71	130 ± 7	0.7 ± 0.1	36 ± 4	<0.1	5.1 ± 0.4	4.8 ± 0.4	<0.5	0.41 ± 0.03	0.9 ± 0.2	8.7 ± 0.4	240 ± 20	<0.05	0.48 ± 0.05	0.21 ± 0.03	<0.5	6.8 ± 0.2	1.4 ± 0.1
ASP-199	300	-	2010.4.2 to 2012.12.18	7.99	22.3	−110	130 ± 7	0.7 ± 0.1	37 ± 3	<0.1	5.5 ± 0.5	5.2 ± 0.5	0.8 ± 0.2	0.43 ± 0.03	0.7 ± 0.2	8.7 ± 0.4	240 ± 20	<0.05	0.49 ± 0.06	0.2	<0.5	6.6 ± 0.2	1.4 ± 0.1

On-site measurements of pH, temperature, and Eh for the seepage groundwater were single-point measurements. Groundwater samples were collected from the 07MI07, 09MI20, and 10MI26 boreholes, and from the A-SP-198 and the A-SP-199 water conducting fractures in excavation walls. mabh, meters along borehole (from collar).

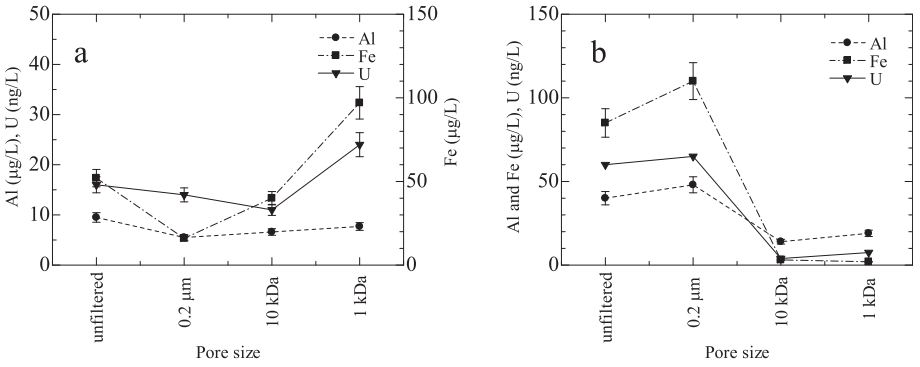

Figure 5 Size-fractionated concentrations of U and colloid-forming elements from the boreholes. Concentrations of U (inverted triangles), Fe (squares), and Al (circles) during groundwater exchange in the **(a)** 09MI20 and **(b)** 10MI26 boreholes.

were 9.5, 5.5, 6.6, and 7.7 μg/L in unfiltered and 0.2 μm, 10 kDa, and 1 kDa filtered groundwaters, respectively. In the case of groundwater sampled from the 10MI26 borehole, Fe and Al were significantly concentrated in unfiltered and 0.2 μm fractions (Figure 5b). The concentrations of Fe were 85, 110, 3.1, and 2.0 μg/L in unfiltered and 0.2 μm, 10 kDa, and 1 kDa filtered groundwaters, respectively, and the concentrations of Al were 40, 48, 14, and 19 μg/L in unfiltered and 0.2 μm, 10 kDa, and 1 kDa filtered groundwaters, respectively.

Table 2 shows the chemical compositions of the filtered groundwater in each sample interval volume from the 09MI20 and 10MI26 boreholes during purging of groundwater by allowing flow-through in the boreholes. Changes in the concentrations of Fe and Al were different in the two boreholes 09MI20 and 10MI26 (Figures 6c,d). For the 09MI20 borehole, the concentrations of Fe and TOC were highest immediately after groundwater purging began (11 μg/L and 1.8 mg/L for Fe and TOC, respectively) and remained approximately constant (3.4 to 4.0 μg/L and 0.8 to 1.3 mg/L for Fe and TOC, respectively) during the purging of 5, 10, and 20 sampling interval volumes of groundwater. Despite the changes in the concentrations of Fe and TOC, the Al concentrations were approximately constant (6.1 ± 0.8 μg/L) during groundwater flow-through in the 09MI20 borehole (Figure 6d). Compared with the 09MI20 borehole, the trend in borehole 10MI26 was different. Although the concentrations of Fe and TOC changed during groundwater flow-through in the 09MI20 borehole, they were approximately constant (2.9 ± 0.4 μg/L and 1.3 ± 0.1 mg/L, respectively) during the flow-through of the groundwater in the 10MI26 borehole (Figure 6b,c). On the other hand, the Al concentration was highest immediately after the replacement of the groundwater began (13 μg/L). The Al concentrations remained approximately constant (5.3 to 7.5 μg/L) during the flow-through of 5, 10, and 20 sampling interval volumes of groundwater.

The chemical compositions of the size-fractionated colloids sampled from fracture seepages on gallery walls (A-SP-198 and A-SP-199) are listed in Table 3. The concentrations of Fe and Al were approximately constant, regardless of filter pore size. The size-fractionated concentrations of Fe were 3.2 to 4.2 μg/L and 3.2 to 3.6 μg/L for fractures A-SP-198 and the A-SP-199, respectively (Figure 7). The concentrations of Fe were almost within the experimental error, i.e., 3.7 ± 0.4 μg/L (1 σ) and 3.5 ± 0.2 μg/L (1 σ) for A-SP-198 and the A-SP-199, respectively. Similar to Fe, the size-fractionated concentrations of Al were approximately constant, but differed significantly between fractures A-SP-198 (18 ± 1 μg/L) and A-SP-199 (9.2 ± 0.3 μg/L) (Figure 7). Although TOC in A-SP-199 was observed in periodic groundwater sampling (Table 1), the size-fractionated concentrations of TOC could not be detected for either of the groundwater seepages, even in the unfiltered fraction (Table 3).

Groundwater chemistry of U and REEs

The size-fractionated concentration of U in unfiltered 09MI20 groundwater (16 ng/L) was slightly higher than those of 0.2 μm and 10 kDa filtered groundwaters at 14 and 11 ng/L, respectively (Figure 5a). The U concentration of 1 kDa filtered groundwater was inconsistent with the size fractionation trend, having the highest value among the sizes (24 ng/L). In the 10MI26 borehole, as well as the changes in Fe and Al concentrations, U was concentrated in unfiltered and 0.2 μm filtered groundwaters (60 and 65 ng/L for unfiltered and 0.2 μm, respectively). The concentrations of U in 10 and 1 kDa filtered groundwaters were 3.9 and 7.5 ng/L, respectively, which were significantly lower compared to those of unfiltered and 0.2 μm filtered groundwaters (Figure 5b).

The concentrations of U were highest immediately after the flow-through of groundwaters began in the sampling intervals. The concentrations were 12 and

Table 2 Changes in the chemical concentrations of colloid-forming elements (Al, Fe, and TOC), REE, and U in the groundwater

Borehole	Sampling date	Interval volumes	V/V_0	Al	Fe	TOC	La	Ce	Pr	Nd	Sm	Eu	Gd	Tb	Dy	Ho	Er	Tm	Yb	Lu	U
				[μg/L]	[μg/L]	[mg/L]	[ng/L]	[ng/L]	[ng/L]	[ng/L]	[ng/L]	[ng/L]	[ng/L]	[ng/L]	[ng/L]	[ng/L]	[ng/L]	[ng/L]	[ng/L]	[ng/L]	[ng/L]
09MI20	2012.10.9	0	0	5.3	11	1.8	4.2	7.6	1.1	4.8	1.3	n.d.	2.1	0.6	4.8	1.6	6.2	0.9	5.6	1.0	12
	2012.10.9	155	5	5.8	4.0	1.3	4.0	8.6	1.2	5.9	1.7	n.d.	2.8	0.8	6.9	2.2	8.5	1.2	7.5	1.4	4.2
	2012.10.10	310	10	6.1	3.6	0.8	3.9	8.3	1.2	5.5	1.7	n.d.	2.6	0.6	5.9	1.8	7.2	0.9	6.4	1.1	2.9
	2012.10.11	620	20	7.3	3.4	0.8	4.3	8.9	1.3	6.2	1.8	n.d.	2.7	0.7	6.2	1.9	7.8	1.1	7.0	1.3	3.7
10MI26	2012.10.9	0	0	13	3.3	1.3	3.5	6.3	0.9	4.2	1.1	n.d.	1.9	0.5	4.8	1.5	5.7	0.8	5.3	0.8	11
	2012.10.9	120	5	7.5	3.1	1.2	3.7	6.6	1.0	4.6	1.4	n.d.	2.0	0.6	5.2	1.6	6.2	0.9	5.5	0.9	4.0
	2012.10.10	240	10	5.7	2.8	1.3	4.0	7.6	1.1	5.2	1.4	n.d.	2.4	0.7	5.6	1.8	6.7	1.0	5.7	0.9	4.2
	2012.10.11	480	20	5.3	2.4	1.3	3.8	7.9	1.2	5.0	1.5	n.d.	2.4	0.6	5.8	1.8	7.0	1.0	6.0	1.0	5.3

V/V_0 indicates the ratio of the total groundwater flow-through volume to the packer volume of the sampling intervals in the boreholes. Ultrafiltration was conducted using 0.2 μm membranes. Groundwater samples were collected during replacement (purging) of the groundwater in the 09MI20 and 10MI26 boreholes.

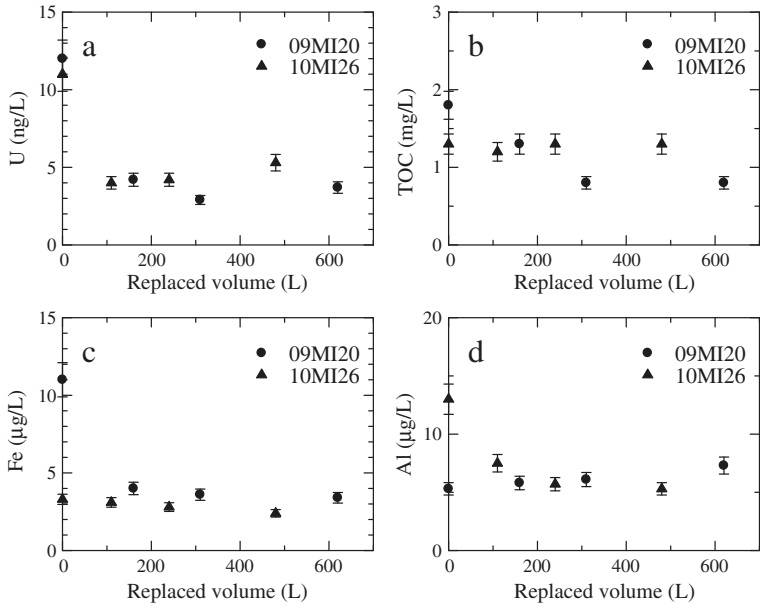

Figure 6 Changes in concentrations of U and colloid-forming elements from the boreholes. The concentrations of **(a)** U, **(b)** TOC, **(c)** Fe, and **(d)** Al during groundwater exchange in the 09MI20 (triangles) and the 10MI26 (circles) boreholes.

11 ng/L in the 09MI20 and 10MI26 boreholes, respectively (Figure 6a). The U concentrations decreased as the groundwater flow-through proceeded in the boreholes, becoming approximately constant (3.7 to 4.2 and 4.0 to 5.3 ng/L for the 09MI20 and the 10MI26 boreholes, respectively) as 5, 10, and 20 sampling interval volumes of groundwater had been replaced. The changes in the U concentrations were similar to those in Fe and TOC in 09MI20 and Al in 10MI26 (Figure 6).

The variations in the size-fractionated chemical concentration of U for the A-SP-198 and the A-SP-199 groundwaters are listed in Table 3. The concentrations of U in the fracture seepages were approximately constant for the various filter pore sizes. The U concentrations in the fracture seepages were comparable to that in the boreholes after 5, 10, and 20 volumes of sampling interval space of groundwater had been replaced (Figures 6 and 7).

Figure 8 shows size-fractionated concentrations of REEs in unfiltered and filtered groundwater sampled from 09MI20 and 10 MI26 boreholes. The concentrations of REEs were higher in the unfiltered fractions of groundwaters sampled from boreholes. The REE concentrations were decreased by ultrafiltration. In contrast to the size-fractionated groundwater and colloid sampling, the groundwater was passed through a 0.2 μm membrane during groundwater flow-through in the sampling interval space in the boreholes. The concentrations of REEs were approximately constant and within analytical error (±10%) during groundwater flow-through in the sampling intervals in the 09MI20 and 10MI26 boreholes (Figure 9).

Changes in the concentrations of REEs in the unfiltered and filtered groundwater sampled from fracture seeps are shown in Figure 10. Similar to the changes in the REE concentrations in the size-fractionated groundwater sampled from boreholes, the above described changes were significantly elevated in the unfiltered fractions of the groundwater seepages (Figures 8 and 10). The REE concentrations decreased with smaller pore size fractions and were approximately constant in 200 to 10 kDa. The higher concentration of REEs in unfiltered groundwaters from boreholes and fracture seepages suggests that REE-bearing material(s) were suspended in the groundwater.

Discussion

Groundwater chemistry in boreholes

Saito et al. (2013) studied the size distribution and elemental compositions of colloids in the MIU groundwater sampled from the 09MI21 borehole located in the −300 m Access/Research Gallery (Figure 2a) using the flow field-flow fractionation (Fl-FFF) technique coupled with an on-line UV/VIS fluorescence detector and ICP-MS analysis. The Fl-FFF analyzed size-fractionated chemical compositions in colloidal materials trapped on the 1 kDa membrane. The size-fractionated compositions of colloids in the 09MI21 groundwater varied among the samples and sizes as follows: (1) the size distributions of Fe overlapped with samples and sizes with a range of 0.5 to 20 nm; (2) Al and Mg had similar size distributions; (3) changes in REE concentrations were correlated with those in Al, Mg, and

Table 3 Size-fractionated chemical concentrations of colloid-forming elements (Al, Fe, and TOC), REE, and U in the groundwater

Location	Sampling date	Pore size	Al	Fe	TOC	La	Ce	Pr	Nd	Sm	Eu	Gd	Tb	Dy	Ho	Er	Tm	Yb	Lu	U
			[μg/L]	[μg/L]	[mg/L]	[ng/L]	[ng/L]	[ng/L]	[ng/L]	[ng/L]	[ng/L]	[ng/L]	[ng/L]	[ng/L]	[ng/L]	[ng/L]	[ng/L]	[ng/L]	[ng/L]	[ng/L]
A-SP-198	2012.9.12	Unfiltered	18	3.2	n.d.	9.1	18	2.2	8.8	2.2	0.1	2.8	0.5	3.5	0.9	2.8	0.3	1.9	0.3	4.5
	2012.9.12	0.2 μm	18	4.2	n.d.	3.7	6.2	0.9	3.7	1.0	0.1	1.4	0.3	2.2	0.7	2.0	0.3	1.5	0.3	1.5
	2012.9.12	200 kDa	18	3.5	n.d.	1.7	3.3	0.5	1.8	0.6	n.d.	0.6	0.1	0.8	0.3	0.8	0.1	0.6	0.2	2.8
	2012.9.12	50 kDa	18	4.1	n.d.	1.1	1.9	0.3	1.1	0.4	n.d.	0.5	0.1	0.8	0.3	0.9	0.2	0.6	0.2	1.3
	2012.9.12	10 kDa	16	3.5	n.d.	1.1	1.7	0.3	1.1	0.3	n.d.	0.5	n.d.	0.8	0.3	0.8	0.2	0.6	0.2	4.9
A-SP-199	2012.9.12	Unfiltered	9.2	3.6	n.d.	3.4	4.5	0.6	2.8	0.9	n.d.	1.5	0.3	2.4	0.6	2.1	0.2	1.3	0.2	2.3
	2012.9.12	0.2 μm	9.4	3.6	n.d.	1.6	2.4	0.4	1.4	0.5	n.d.	0.6	0.2	1.1	0.4	1.1	0.2	0.7	0.2	2.0
	2012.9.12	200 kDa	9.7	3.6	n.d.	1.2	1.9	0.4	1.1	0.4	n.d.	0.5	0.1	0.9	0.3	1.0	0.2	0.7	0.2	2.1
	2012.9.12	50 kDa	9.1	3.7	n.d.	1.5	2.3	0.4	1.4	0.4	n.d.	0.5	0.1	1.1	0.4	1.1	0.2	0.8	0.2	1.1
	2012.9.12	10 kDa	9.0	3.2	n.d.	0.7	1.0	0.2	0.7	0.2	n.d.	0.3	n.d.	0.6	0.2	0.6	0.1	0.5	0.2	0.92

Groundwater samples were collected from A-SP-198 and A-SP-199 fractures.

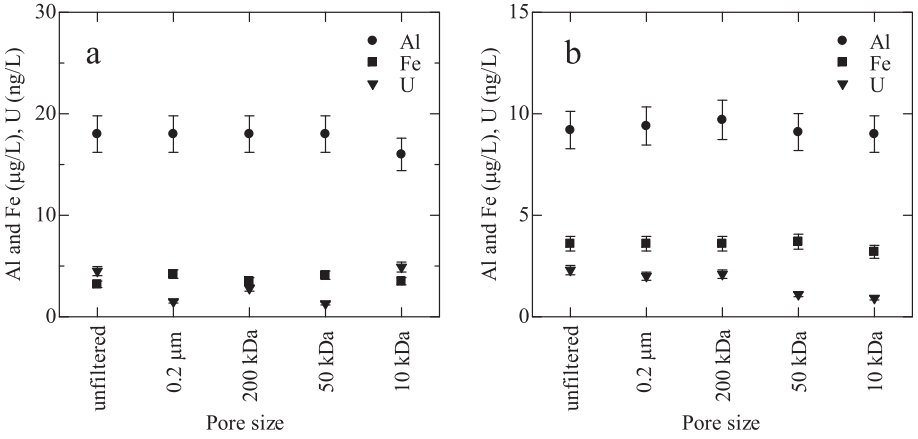

Figure 7 Size-fractionated concentrations of colloid-forming elements from underground fracture seepages. Fe (squares) and Al (circles), and U (inverted triangle) for the **(a)** A-SP-198 and **(b)** A-SP-199 fractures.

organic colloids; and (4) size distributions of U corresponded to those of REEs.

In the present study, size fractionations of groundwater samples with colloids were conducted by ultrafiltration. In general, suspended particles in groundwater were removed by ultrafiltration. However, colloids having particle sizes smaller than the membrane pore size can pass through the filter and mix in the filtrate. The concentrations of colloid-forming elements in the filtrate apparently change according to the colloid penetration.

The size-fractionated concentrations of Fe in the 09MI20 borehole varied with the pore size (Figure 5). The Fe concentration of the 1 kDa filtered groundwater was higher than that of the unfiltered sample. The possible reason for the higher concentration in the filtered groundwater compared to the unfiltered groundwater can be explained by the natural variation of groundwater chemistry during sampling and/or experimental contamination by colloids in the filtrate. For the groundwater sampling from boreholes, anthropogenic precipitation(s)

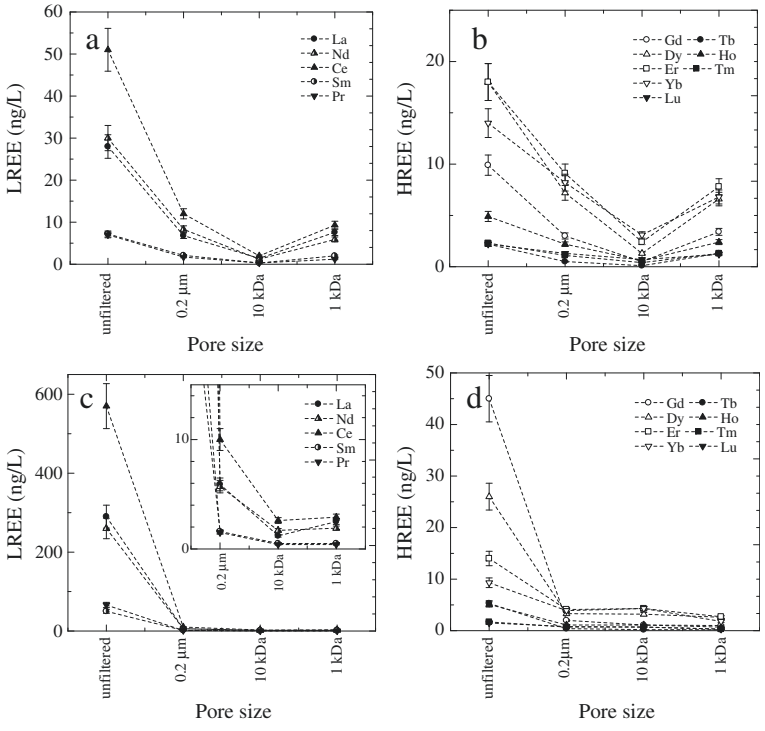

Figure 8 Size-fractionated concentrations of REEs from boreholes. (a) LREE and **(b)** HREE in the 09MI20 borehole and **(c)** LREE and **(d)** HREE in the 10MI26 borehole.

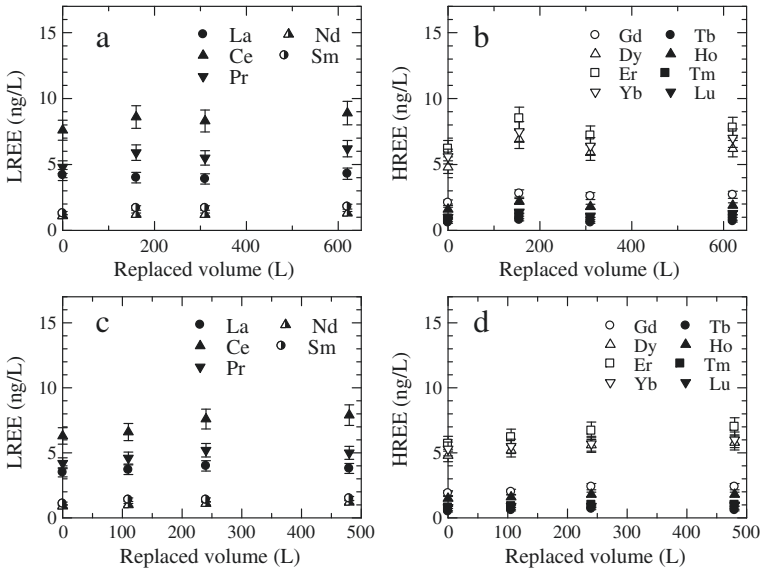

Figure 9 Changes in REE concentration during replacement of the groundwater from the boreholes. (a) LREE and **(b)** HREE in the 09MI20 borehole, and **(c)** LREE and **(d)** HREE in the 10MI26 borehole.

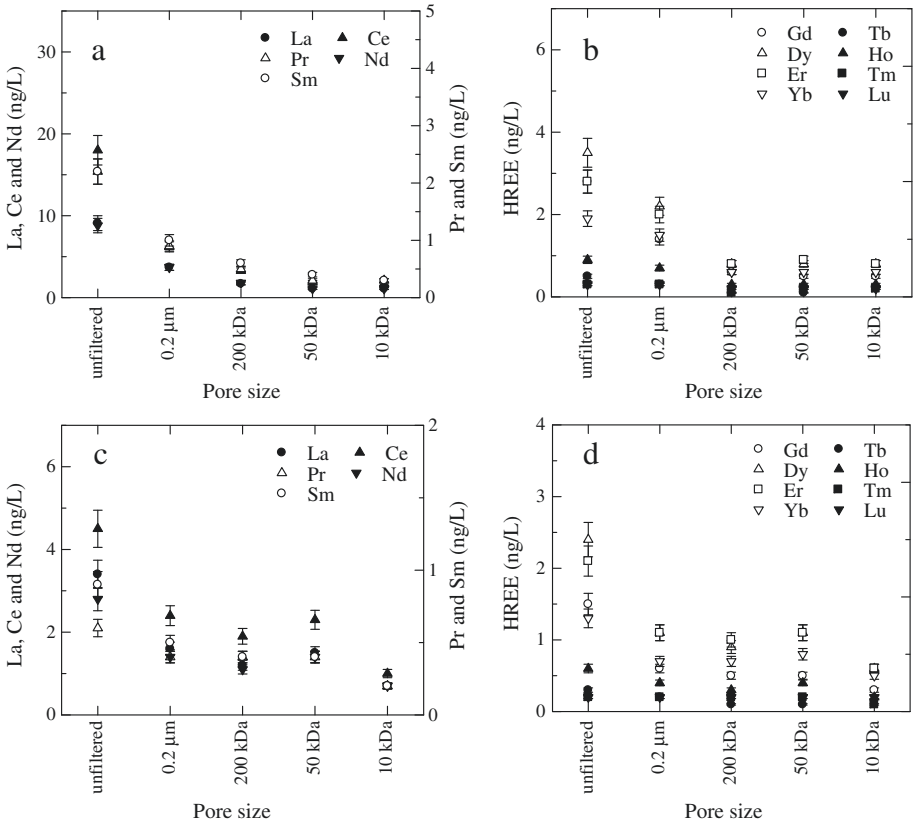

Figure 10 Size-fractionated concentrations of REEs from water-conducting fractures in excavation walls. (a) LREE and **(b)** HREE in the ASP-198 fracture, and **(c)** LREE and **(d)** HREE in the ASP-199 fracture.

was observed by BTV (Figure 1b). Since the major concern with the mobilization of colloids is rapid groundwater pumping, it is recommended that the pumping rate be kept low, to a maximum of approximately 100 mL/min (Ryan and Elimelech 1996). In the present case of groundwater sampling using hydrochemical monitoring systems, the groundwater flow rate attained was approximately 1 L/min. Consequently, the deviation in the fractionated concentration of Fe can be attributed to the mobilization of colloids in the borehole.

The concentration of Fe in the filtered groundwater changed with the replacement of groundwater in the sampling-intervals (Figure 6). Moreover, size fractionation by ultrafiltration may cause a change in the quantity of the colloidal material that passed through the 0.2 μm membrane and/or the aqueous concentration. In general, the source of aqueous Fe can be the dissolution of biotite, chlorite, and smectite (Acker and Bricker 1992). The deeper groundwater is significantly reduced (Table 1). However, Fe hydroxides such as goethite are precipitated on fractures and mineral surfaces in the granite (Iwatsuki and Yoshida 1999). Sugimori et al. (2008) described the weathering processes of biotite and chlorite in the Toki granite. Iron (oxy-)hydroxides such as ferrihydrite and goethite can precipitate depending on the pO_2 or Eh.

We calculated saturation indices ($SI = \log IAP/K_{sp}$; [IAP, ion activity product; K_{sp}, solubility product]) for Fe-bearing minerals using the program REACT from 'The Geochemist's Workbench' (Bethke 1992) with the thermodynamic database 'thermo.com.v8.r6 + .dat'. Immediately after groundwater replacement began, the groundwater was supersaturated with respect to high Fe-bearing smectite (SI = 0.03) and low Fe-bearing smectite (SI = 0.03 and 0.52), while they became undersaturated (SI = −0.03 and −0.80) after 20 sampling interval volumes of groundwater were replaced. If Fe-bearing phase(s) passed through the membrane, the filtrate should be in equilibrium and/or oversaturated with respect to corresponding solid phase(s). The high Fe concentration immediately after groundwater purging was the result of Fe-bearing colloids being flushed out and contaminating the filtrate. Based on SEM observations, Fe-bearing aluminosilicates with a diameter of 100 nm were collected on the membrane in the 09MI20 groundwater (Figure 3). Tsubaki et al. (2012) reported that aggregations of nanoparticles can be trapped by a membrane. Accordingly, the aggregation of colloids explains the trapping of Fe-bearing aluminosilicates on the membrane. Fe-bearing aluminosilicate in the 09MI20 groundwater (Figure 3) was identified by thermodynamic calculation as Fe-bearing smectite. Such precipitation may be released to groundwater and mobilized by water pressure fluctuations during sampling. The 'mobilized' Fe-bearing colloids affect the concentration of Fe by passing through the membrane. The concentrations of Fe in the borehole and fracture seeps were comparable (Figures 6c and 7). Consequently, the Fe-bearing colloids were flushed out with the groundwater from inside the borehole during removal of the groundwater in the borehole. Thus, the variation in the size-fractionated concentration of Fe in 09MI20 can be explained by the contamination by secondary Fe-bearing colloids formed in the borehole after drilling.

For the size-fractionated groundwater sampled from the 10MI26 borehole, Fe and Al were concentrated in unfiltered and 0.2 μm filtered groundwater, whereas the concentrations were very low in 10 and 1 kDa filtered groundwater. The 10 kDa MWCO corresponds to a pore size of 6.3 nm. Consequently, the Fe-bearing and Al-bearing colloids of 0.2 μm to 6.3 nm in size were present in the borehole groundwater. The concentration of Al changed during removal of groundwater from the 10MI26 borehole. Immediately after groundwater removal began, the filtered groundwater was supersaturated with respect to several tens of Al-bearing minerals, kaolinite, low Fe-bearing smectite, pyrophyllite, etc. After purging 20 borehole volumes, the groundwater became undersaturated with respect to low Fe-bearing smectite and pyrophyllite. The high Al concentration immediately after groundwater purging was the result of Al-bearing colloids being flushed out and contaminating the filtrate. Accordingly, the filtered groundwater was supersaturated with respect to the low Fe-bearing smectite and pyrophyllite in the initial sampling. After elimination of the mobilized Al-bearing phase(s), the groundwater became undersaturated with respect to the Al-bearing phase(s) and large portions of the Al-bearing phase(s) were flushed out during the groundwater purging. The colloids and secondary minerals adhering to the borehole walls were mobilized by fluctuating water pressures during borehole sampling. These were unavoidable processes in some uncertainties in the research on colloids in groundwater.

Nevertheless, groundwater sampling from boreholes has the significant advantage of *in situ* sample collection. At least, the concentrations of Fe, Al, and TOC changed during purging of groundwater from boreholes. The colloids were likely mobilized by fluctuations in water pressure during sampling. For quality control of groundwater and colloid sampling from boreholes, the presence of anthropogenic colloids can be mitigated to some extent by pumping out or flushing the groundwater from a borehole by removing several volumes of groundwater from the packer isolated sampling intervals in the borehole.

Groundwater chemistry of size-fractionated fracture seepage

In the Toki granite, groundwater flow is fracture-controlled (joints and faults) (Illman et al. 2009). Hence, groundwater from both boreholes and seepage passed through the granitic fractures and/or fracture networks. The concentrations of major constituents in the groundwater seepages in the −300 m gallery were different from the concentrations in the 09MI20 borehole groundwater, even though both sample locations are at the same depth (Table 1). Around the study area, the groundwater chemistry is Na-Ca-HCO_3 type at shallow depths, whereas it is Na-(Ca)-Cl type at deep levels (Iwatsuki et al. 2005). Although the concentration of Cl^- in borehole groundwater increased with depth, that in the groundwater seepages were higher than in boreholes at the same depth (−300 m) (Table 1). The sampling locations of boreholes are sandwiched between the main shaft and the ventilation shaft (Figure 2), and thus the underground conditions were depressurized vertically as shaft construction progressed (Mizuno et al. 2013). In contrast, the fracture seepages are located in the horizontal −300 m access/research gallery (Figure 2). Consequently, the groundwater sources for the boreholes and the fracture seepages on the gallery wall were likely different.

For the groundwater seepage from fractures in galleries, the colloid-forming elements, Fe and Al, are likely to be present as aqueous (complex) ions in the groundwater flowing in fractures (Figure 7). In the Toki granite, montmorillonite and chlorite occur as fracture-filling minerals (Iwatsuki and Yoshida 1999). The differences in the Al concentrations can be accounted for by the variation of fracture-filling minerals. The groundwater seepage was supersaturated with respect to beidellite in the A-SP-199 fracture, but was undersaturated in the A-SP-198 fracture. The saturation index for Al-bearing minerals in the fractures, the Mg-bearing smectite group, and illite could not be calculated because the Mg concentration is too low, i.e., below the detection limit (Table 3). Since the mobile Fe-bearing and Al-bearing colloids were uncommon in the groundwater from the fracture seepages, the natural Fe-bearing and Al-bearing colloids may be negligible in the groundwater in fractures. The groundwater sampled from seepages was free of contamination by anthropogenic materials. The groundwater sampling from the water-conducting fractures is suitable for water quality control of colloid issues.

Distribution of U on colloids

Changes in the size-fractionated concentrations of U in groundwater from the 09MI20 and 10MI26 boreholes are associated with similar changes in concentration of Fe and Al (Figure 5). For the 09MI21 borehole, the size distributions of U correspond to those of Al and organic matter (Saito et al. 2013). In the present study, the U association with Al for the 10MI26 is consistent with that for borehole 09MI21. In addition, the U concentration is associated with the Al and Fe in the 10MI26 groundwater. The U concentrations decreased at an approximately constant rate as groundwater replacement proceeded in the boreholes (Figures 5 and 6). Although aqueous U forms strong carbonate complexes (Waite et al. 1994), alkalinity was constant during the groundwater flushing in the boreholes (1.24 and 1.15 meq/L for the 09MI20 and 10MI26 boreholes, respectively). Saturation indices for U-bearing minerals, such as uraninite (UO_2) during flushing of the groundwaters were −1.0 to −1.5 and −1.0 to −1.3 in the 09MI20 and 10MI26 boreholes, respectively. The groundwaters were undersaturated with respect to the U-bearing minerals. Accordingly, U-bearing intrinsic colloids cannot occur in the groundwater. The changes in the U concentrations were similar to those in Fe and TOC in the 09MI20 borehole and Al in the 10MI26 borehole (Figure 6). The association of U with Fe-bearing, Al-bearing, and organic colloids resulted in the contamination of the filtered groundwater. The size distributions of U-bearing colloids correspond to those of Al-bearing colloids and organic colloids (Saito et al. 2013). The change in U concentration along with the concentrations of Al was consistent with the size fractionation by Fl-FFF. In addition, Fe-bearing and/or organic colloids of diameter <0.2 μm affected the sampling quality of the groundwater.

The size-fractionated chemical compositions of U for the A-SP-198 and A-SP-199 groundwaters are approximately constant, irrespective of filter size. If the U moves with colloids of various particle sizes, the U concentrations should decrease as the pore size decreases. However, the U concentrations were approximately constant regardless of pore size. Thus, the uranium migration by colloidal phases in groundwater fracture flow was not identified in the present study.

Distribution of REEs on colloids

The size-fractionated concentrations of REEs in borehole groundwaters decreased significantly as membrane pore sizes decreased (Figure 8). The REE concentrations of unfiltered groundwater were approximately ten times higher than that of 0.2 μm filtered groundwater. The correlation between size-fractionated concentration of REEs and Al and Fe were not observed in the boreholes (Figures 5 and 8). In contrast, the concentrations of REEs were approximately constant during groundwater replacement in the sampling intervals in the 09MI20 and 10MI26 boreholes (Figure 9). The transport of REEs associated with Fe-bearing and Al-bearing colloids was not observed (Figures 6 and 9). Ultrafiltration was

conducted using a 0.2 μm membrane during groundwater flow-through in the sampling intervals in the boreholes. The independence of REE concentrations on groundwater replacement suggested that the >0.2 μm REE-bearing colloids in the groundwater were almost completely trapped on the 0.2 μm membrane. In addition to the borehole groundwater, the concentrations of REEs are significantly higher in unfiltered groundwater from fracture seepages (Figure 10). The REE concentrations decreased with decreasing pore size fractions, which were approximately constant from 200 to 10 kDa. The 200 kDa of MWCO membrane corresponds to a pore size of approximately 100 nm. The mobile Fe-bearing and Al-bearing colloids are rare in the groundwater from fracture seepages (Figure 7). Consequently, the mobility of REEs was scarcely facilitated by Fe-bearing and Al-bearing colloidal materials. The >0.2 μm REE-bearing particles were transported in the MIU groundwater. Iida et al. (1998) investigated REE-bearing minerals in the Toki granite, bastnaesite ((LREE)CO_3F), and parasite ($Ca(LREE)_2(CO_3)_3F_2$), which are several hundreds to tens of micrometers in size. Thus, the large REE-bearing mineral(s) were potentially removed from the groundwater by the 0.2 μm membrane. In the present study, REE-bearing mineral(s) suspended in the groundwater cannot be directly observed by SEM observation because of the very low concentration of colloids in groundwater. The REE-bearing particles are mobile in groundwater sampled from both borehole and fracture seepages (Figures 8 and 10).

The chemical properties of REEs, especially LREEs, are comparable to those of transuranic elements due to the similarities in ionic radii, oxidation state, and complexation with anions (Krauskopf 1986). Chondrite-normalized REE patterns of size-fractionated groundwater sampled from boreholes are shown in Figure 11. For the unfiltered 09MI20 groundwater, the REE pattern has a downward convex shape in the middle REE (MREE), which was notable for filtered groundwater (Figure 11a). The REE pattern of unfiltered 10MI26 groundwater was significantly different from those of the filtered groundwaters. The unfiltered 10MI26 groundwater was enriched with LREE (Figure 11b). The REE-bearing materials were suspended in the groundwater and affected the REE pattern of the unfiltered groundwater. In contrast, the REE patterns of filtered groundwater were enriched in heavy REE (HREE), which was comparable to the patterns during groundwater replacement.

Figure 12 shows chondrite-normalized REE patterns of the filtered groundwaters during groundwater replacement in the borehole. Although the concentrations of Fe, Al, and TOC for the filtered groundwater changed, the REE patterns in the groundwaters did not change during the groundwater flow-through in the boreholes and were significantly enriched in HREEs. In CO_2-rich and pH-neutral groundwater, HREEs are enriched due to the REE carbonate aqueous complex (Négrel et al. 2000). In the present study, REE aqueous species were calculated using 'The Geochemist's Workbench' (Bethke 1992), which revealed that the predominant REE species were $REE(CO)_3^+$ in all filtered groundwater. The Takahashi et al. (2002) study revealed that the REEs in the groundwater (approximately 150 mbgl) are dissolved carbonate complexes from the Toki granite. The HREE enrichment in the groundwater can be explained by the formation of carbonate complexes.

With respect to borehole sampling, anthropogenic colloids and secondary mineral(s) precipitated on the borehole walls (Figure 1). The anthropogenic colloids formed in the borehole were flushed out during groundwater flow-through (Figure 6). However, the mobility of REEs in the borehole groundwater did not change with the mobilized Fe-bearing, Al-bearing, and organic colloids. Sholkovitz (1992) studied the mobility of REEs associated with colloids in river water. The REE patterns of the river water and those of colloids are enriched in

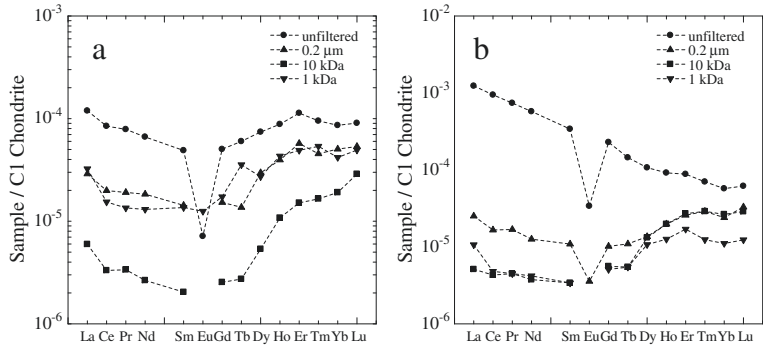

Figure 11 Chondrite-normalized REE patterns of the unfiltered groundwater and filtered groundwater with different pore sizes. Chondrite data are from Anders and Grevesse (1989). Unfiltered (circles), 0.2 μm (triangles), 10 kDa (squares), and 1 kDa (inverted triangles) in the **(a)** 09MI20 and **(b)** 10MI26 boreholes.

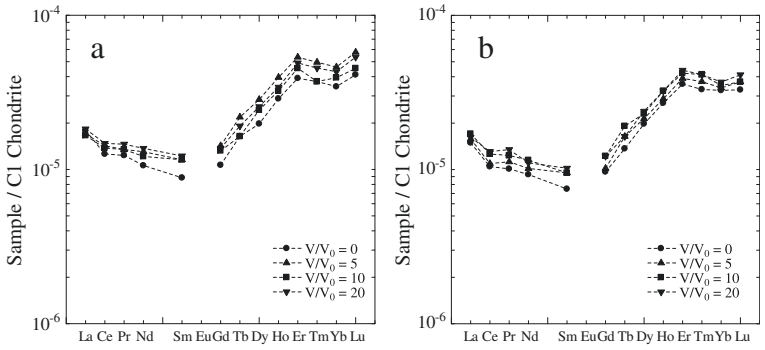

Figure 12 Chondrite-normalized REE patterns of the groundwater during development of the (a) 09MI20 and (b) 10MI26 boreholes. Chondrite data are from Anders and Grevesse (1989). V/V_0 is the ratio of the replaced volume of the groundwater to the sampling interval volume in the boreholes.

HREE and LREE, respectively. The enrichment of LREE in unfiltered groundwater and HREE in filtered groundwater is in agreement with the river colloid samples. In the present study, REE carriers are the <0.2 μm REE bearing particles.

For the groundwater sampled from fractures, chondrite-normalized REE patterns of unfiltered and size-fractionated filtered groundwaters are shown in Figure 13. The REE pattern of the unfiltered groundwater for A-SP-198 was slightly enriched in LREE. In contrast, the REE pattern of the filtrate was almost flat from the lightest REE (La) to the heaviest REE (Lu). For A-SP-199, because of a small change in the concentrations of REEs in the unfiltered and filtered groundwater (Figure 10), changes in the REE patterns by REE-bearing particles were not observed (Figure 13b). The REE-bearing materials are mainly >0.2 μm in size in the groundwater sampled from underground fracture seeps (Figure 10). Accordingly, the REE patterns of unfiltered groundwater probably exhibit a mixture of the groundwater and REE-bearing solid materials. In addition to the borehole sampling, the enrichment of LREEs in the unfiltered groundwater may be accounted for by the contamination of LREE-enriched natural colloidal materials (>0.2 μm) in the groundwater. The mobility of REEs was only slightly facilitated by the Fe-bearing and Al-bearing colloids. Consequently, the REE-bearing materials that originated from the source granite were transported in a continuous groundwater inflow system.

Conclusions

We investigated colloids and their association with analogue elements at the Mizunami Underground Research Laboratory. Groundwater was sampled from underground boreholes and gallery walls, and the colloids were separated by size-fractionated ultrafiltration. The major findings and conclusions are as follows:

1) U was associated with Al-bearing colloids, Fe-bearing colloids, and organic matter.
2) REE-bearing material(s) >0.2 μm were mobile in deep granitic groundwater.
3) Groundwater sampling from water-conducting fractures in host rock and colloid elimination in boreholes are important components of water quality control in geochemical investigations.

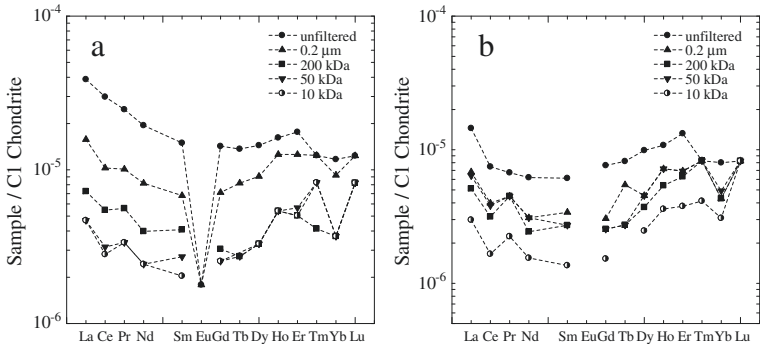

Figure 13 Chondrite-normalized REE patterns of the unfiltered groundwater and filtered groundwater with different pore sizes. Chondrite data are from Anders and Grevesse (1989). **(a)** A-SP-198 and **(b)** A-SP-198 fracture seeps.

Abbreviations
BTV: borehole televiewer; EDS: energy-dispersive X-ray spectrometry; Fl-FFF: flow field-flow fractionation; HREE: heavy REE; JAEA: Japan Atomic Energy Agency; LREE: light REE; MIU: Mizunami Underground Research Laboratory; REE: rare earth elements; SEM: scanning electron microscopy; URL: underground research laboratory.

Competing interests
The authors declare that they have no competing interests.

Authors' contributions
TM carried out microscopic analysis, interpreted the data, drafted the paper. KO carried out groundwater sampling and chemical analysis. TI designed and directed the study and helped to draft the paper. All authors read and approved the final manuscript.

Acknowledgements
We would like to thank Dr. K. Umeda, convener of the session 'Geological Disposal of Radioactive Waste and Earth Science' at the Japan Geoscience Union Meeting 2013 for recommending invited research articles based on a presentation at the annual meeting. The technical comments and English review by Mr. G. McCrank, an ex-JAEA International Fellow, are appreciated. The quality of our manuscript has been significantly improved by valuable comments from three anonymous reviewers.

Received: 8 January 2014 Accepted: 12 November 2014
Published online: 12 December 2014

References
Abdel-Fattah AI, Zhou D, Boukhalfa H, Tarimala S, Ware SD, Keller AA (2013) Dispersion stability and electrokinetic properties of intrinsic plutonium colloids: implications for subsurface transport. Environ Sci Technol 47:5626–5634
Acker J, Bricker OP (1992) The influence of pH on biotite dissolution and alteration kinetics at low temperature. Geochim Cosmochim Acta 56:3073–3092
Anders E, Grevesse N (1989) Abundances of the elements: meteoric and solar. Geochim Cosmochim Acta 53:197–214
Aosai D, Yamamoto Y, Mizuno T (2010) Development of new ultrafiltration techniques maintaining in-situ hydrochemical conditions for colloidal study. The 13th International conference on environmental remediation and radioactive waste management, Tsukuba, Japan, October 2010. ICEM2010-40072
Bau M (1999) Scavenging of dissolved yttrium and rare earths by precipitating iron oxyhydroxide: experimental evidence for Ce oxidation, Y-Ho fractionation, and lanthanide tetrad effect. Geochim Cosmochim Acta 63:67–77
Bethke C (1992) The geochemist's workbench: a user's guide to Rxn, Act2, Tact, React, and Gtplot
Buddemeier RW, Hunt JR (1988) Transport of colloidal contaminants in groundwater: radionuclide migration at the Nevada test site. Appl Geochem 3:535–548
Claveranne-Lamolère C, Aupiais J, Lespes G, Frayret J, Pili E, Pointurier F, Potin-Gautier M (2011) Investigation of uranium-colloid interactions in soil by dual field-flow fractionation/capillary electrophoresis hyphenated with inductively coupled plasma-mass spectrometry. Talanta 85:2504–2510
Coppin F, Berger G, Bauer A, Castet S, Loubet M (2002) Sorption of lanthanides on smectite and kaolinite. Chem Geol 182:57–68
Davis JA, Kent DB (1990) Surface complexation modeling in aqueous geochemistry. Rev Mineral 23:177–260
Degueldre C, Triay I, Kim JI, Vilks P, Laaksoharju M, Miekeley N (2000) Groundwater colloid properties: a global approach. Appl Geochem 15:1043–1051
Dia A, Gruau G, Olivié-Lauquet G, Riou C, Molénat J, Curmi P (2000) The distribution of rare earth elements in groundwaters: assessing the role of source-rock composition, redox changes and colloidal particles. Geochim Cosmochim Acta 64:4131–4151
Dideriksen K, Christiansen BC, Baker JA, Frandsen C, Balic-Zunic T, Tullborg E, Mørup S, Stipp SLS (2007) Fe-oxide fracture fillings as a palæo-redox indicator: structure, crystal form and Fe isotope composition. Chem Geol 244:330–343
Dzombak DA, Morel FMM (1990) Surface complexation modeling: hydrous ferric oxide, 393rd edn. Wiley, New York
Filella M, Chanudet V, Philippo S, Quentel F (2009) Particle size and mineralogical composition of inorganic colloids in waters draining the adit of an abandoned mine, Goesdorf, Luxembourg. Appl Geochem 24:52–61
Flury M, Qiu H (2008) Modeling colloid-facilitated contaminant transport in the vadose zone. Vadose Zone J 7:682–697
Hochella MF, Lower SK, Maurice PA, Penn RL, Sahai N, Sparks DL, Twining BS (2008) Nanominerals, mineral nanoparticles, and earth systems. Science 319:1631–1635
Iida Y, Ohnuki T, Isobe H, Yanase N, Sekine K, Yoshida H, Yusa Y (1998) Hydrothermal redistribution of rare earth elements in Toki granitic rock, central Japan. J Contam Hydrol 35:191–199
Illman WA, Liu X, Takeuchi S, Yeh T-CJ, Ando K, Saegusa H (2009) Hydraulic tomography in fractured granite: Mizunami underground research site, Japan. Water Resour Res 45:W01406
Iwatsuki T, Yoshida H (1999) Groundwater chemistry and fracture mineralogy in the basement granitic rock in the Tono uranium mine area, Gifu Prefecture, Japan—Groundwater composition, Eh evolution analysis by fracture filling minerals. Geochem J 33:19–32
Iwatsuki T, Furue R, Mie H, Ioka S, Mizuno T (2005) Hydrochemical baseline condition of groundwater at the Mizunami underground research laboratory (MIU). Appl Geochem 20:2283–2302
Kanai Y (2011) Study on the analysis of colloidal materials by ultrafiltration method (Study on elucidation and characterization of colloid (part 3)). Bull Geol Surv Japan 62:371–388
Kersting AB, Efurd DW, Finnegan DL, Rokop DJ, Smith DK, Thompson JL (1999) Migration of plutonium in ground water at the Nevada test site. Nature 397:56–59
Krauskopf KB (1986) Thorium and rare-earth metals as analogs for actinide elements. Chem Geol 55:323–335
Kulaksız S, Bau M (2013) Anthropogenic dissolved and colloid/nanoparticle-bound samarium, lanthanum and gadolinium in the Rhine River and the impending destruction of the natural rare earth element distribution in rivers. Earth Planet Sci Lett 362:43–50
Mahoney JJ, Cadle SA, Jakubowski RT (2009) Uranyl adsorption onto hydrous ferric oxides—a re-evaluation for the diffuse layer model database. Environ Sci Technol 43:9260–9266
McCarthy JF, Zachara JM (1989) Subsurface transport of contaminants. Environ Sci Technol 23:496–502
Metcalfe R, Takase H, Sasao E, Ota K, Iwatsuki T, Arthur RC, Stenhouse MJ, Zhou W, Mackenzie AB (2006) A system model for the origin and evolution of the Tono Uranium Deposit, Japan. Geochem: Explor Environ Anal 6:13–31
Mizuno T, Aosai D, Shingu S, Hagiwara H, Yamamoto Y, Fukuda A (2013) Hydrochemical changes associated with construction of Mizunami underground research laboratory. Trans At Energy Soc Jpn 12:89–102
Neck V, Kim JI (2001) Solubility and hydrolysis of tetravalent actinides. Radiochim Acta 89:1–16
Négrel P, Guerrot C, Cocherie A, Azaroual M, Brach M, Fouillac C (2000) Rare earth elements, neodymium and strontium isotopic systematics in mineral waters: evidence from the Massif Central, France. Appl Geochem 15:1345–1367
Novikov AP, Kalmykov SN, Utsunomiya S, Ewing RC, Horreard F, Merkulov A, Clark SB, Tkachev VV, Myasoedov BF (2006) Colloid transport of plutonium in the far-field of the Mayak Production Association, Russia. Science 314:638–641
Opiso E, Sato T, Yoneda T (2009) Adsorption and co-precipitation behavior of arsenate, chromate, selenate and boric acid with synthetic allophane-like materials. J Hazard Mater 170:79–86
Pokrovsky OS, Viers J, Shirokova LS, Shevchenko VP, Filipov AS, Dupré B (2010) Dissolved, suspended, and colloidal fluxes of organic carbon, major and trace elements in the Severnaya Dvina River and its tributary. Chem Geol 273:136–149
Raiswell R (2011) Iron transport from the continents to the open ocean: the aging-rejuvenation cycle. Elements 7:101–106
Ryan JN, Elimelech M (1996) Colloid mobilization and transport in groundwater. Colloid Surface A 107:1–56
Saito T, Suzuki Y, Mizuno T (2013) Size and elemental analyses of nano colloids in deep granitic groundwater: implications for transport of trace elements. Colloid Surface A 435:48–55
Sasao E, Ota K, Iwatsuki T, Niizato T, Arthur RC, Stenhouse MJ, Zhou W, Metcalfe R, Takase H, Mackenzie AB (2006) An overview of a natural analogue study of the Tono uranium deposit, central Japan. Geochem Explor Environ Anal 6:5–12
Sholkovitz ER (1992) Chemical evolution of rare earth elements: fractionation between colloidal and solution phases of filtered river water. Earth Planet Sci Lett 114:77–84
Sholkovitz ER, Landing WM, Lewis B (1994) Ocean particle chemistry: the fractionation of rare earth elements between suspended particles and seawater. Geochim Cosmochim Acta 58:1567–1579

Stefánsson A (2007) Iron(III) hydrolysis and solubility at 25°C. Environ Sci Technol 41:6117–6123
Sugimori H, Iwatsuki T, Murakami T (2008) Chlorite and biotite weathering, Fe^{2+}-rich corrensite formation, and Fe behavior under low pO_2 conditions and their implication for Precambrian weathering. Am Mineral 93:1080–1089
Takahashi Y, Yoshida H, Sato N, Hama K, Yusa Y, Shimizu H (2002) W- and M-type tetrad effects in REE patterns for water-rock systems in the Tono uranium deposit, central Japan. Chem Geol 184:311–335
Tsang CF, Hufschmied P, Hale FV (1990) Determination of fracture inflow parameter with a borehole fluid conductivity logging method. Water Resour Res 26:561–578
Tsubaki H, Saito T, Murakami T (2012) Size distribution of ferrihydrite aggregate and its implication for metal adsorption and transport. J Mineral Petrol Sci 107:244–249
Tsukimura K, Suzuki M, Suzuki Y, Murakami T (2010) Kinetic theory of crystallization of nanoparticles. Cryst Growth Des 10:3596–3607
Utsunomiya S, Kersting AB, Ewing RC (2009) Groundwater nanoparticles in the far-field at the Nevada test site: mechanism for radionuclide transport. Environ Sci Technol 43:1293–1298
Waite TD, Davis JA, Payne TE, Waychunas GA, Xu N (1994) Uranium(VI) adsorption to ferrihydrite: application of a surface complexation model. Geochim Cosmochim Acta 58:5465–5478
Wang Y, Frutschi M, Suvorova E, Phrommavanh V, Descostes M, Osman AAA, Geipel G, Bernier-Latmani R (2013) Mobile uranium(IV)-bearing colloids in a mining-impacted wetland. Nat Commun 4:2942
Willis SS, Johannesson KH (2011) Controls on the geochemistry of rare earth elements in sediments and groundwaters of the Aquia aquifer, Maryland, USA. Chem Geol 285:32–49

doi:10.1186/s40645-014-0028-z
Cite this article as: Munemoto *et al.*: Distribution of U and REE on colloids in granitic groundwater and quality-controlled sampling at the Mizunami underground research laboratory. *Progress in Earth and Planetary Science* 2014 **1**:28.